



University Mohamed Khider of Biskra
Faculty of Sciences and Technologie
Department of Mechanical Engineering

MASTER'S THESIS

Domain: Sciences and Techniques
Sector: Mechanical Engineering
Specialty: Metallurgy

Ref. : Entrez la référence du document

Presented by :
Talal KHIREDINE

Monday 26 MAI 2025

Use of date as a green inhibitor in HCl medium for carbon steel

Jury :

Dr	DJELLAB Mounir	MCA	Université de Biskra	President
Pr	BENTRAH Hamza	PR	Université de Biskra	Rapporteur
M	LAMMADI Fatima Zohra	MCB	Université de Biskra	Examinator

Academic Year : 2024 - 2025

ACKNOWLEDGMENTS

*First, we thank God for helping us achieve success. With all due respect and thanks to our supervisor, **Pr. Hamza Bentrah**, for his assistance, guidance, and support during the completion of this study.*

*We sincerely thank the jury president, **Dr. Mounir DJALLAB**, and the examiner, **Dr. Fatima Zohra Lamadi**, who kindly agreed to judge our work. We also thank all the managers and staff of our Mechanical Engineering Department, and all the participants in our training. Finally, we would like to express our gratitude to all our friends and colleagues, and all those who helped us directly or indirectly during the completion of this work.*

Thank you...

I dedicate this modest work to

My mother, whose prayers have always accompanied me in completing this work.

To

My father, whose courage and love inspired me to continue this work.

To

My sisters Aicha, Bassmala, and Alaâ.

To

My brothers Mohamed, Abdelrahmen, Mortadha, and Asil.

To my friend in my study path Arriech Ahmed Wadie

To all my friends and colleagues.

To those who wish me a future full of joy, success, and happiness.

LISTS OF FIGURES

Figure (I.1) :	corrosion of an aluminum bronze valve by concentrated HCl	5
Figure (I.2) :	Exemple of corrosion with H ₂ SO ₄	7
Figure (I.3) :	corrosion of iron in acidic medium.....	8
Figure (I.4) :	Diagramme potentiel-ph of iron (T=25 C°).the concentration dissolved ionic species C _{Fe3+} et C _{Fe2+} vaut 10 ⁻⁶ mol/L	10
Figure (I.5) :	Variation of corrosion rate as a function of pH	11
Figure (I.6) :	(a) Localized corrosion (b) Homogeneous corrosion of a metal.....	12
Figure (I.7) :	Pitting corrosion of stainless steel	13
Figure (I.8) :	Initiation (a) and propagation (b) of a sting	16
Figure (I.9) :	Classification of corrosion inhibitors.....	18
Figure (II.1) :	Metallographic structure of API 5L X70 carbon steel produced after 2% nital attack.....	21
Figure (II.2) :	The molecular structure of galacturonic acid	25
Figure (II.3) :	Photograph of the electrochemical measuring device	26
Figure (III.1) :	Polarization curves of API 5 L X70 steel in 0.5 M HCl medium at 25°C, (a) linear curve, (b) logarithmic curve.....	30
Figure (III.2) :	Morphology of corrosion of API 5L X70 steel observed by SEM in HCl environments (immersion time: 72 hours).....	31
Figure (III.3) :	Potentiodynamic polarization curves for API 5L X70 pipeline steel in 0.5 M HCl without and with different concentrations of GDE at 20°C.....	33
Figure (III.4) :	EIS plots for API 5L X70 pipeline steel 0.5 M HCl medium with and without different concentration of GDE at 20°C, Nyquist.....	35
Figure (III.5) :	Simulated and experimental impedance diagrams of API5L X42 pipeline steel with equivalent circuit in hydrochloric acid medium.....	37
Figure (III.6) :	Langmuir adsorption isotherm of GDE on the surface of API 5L X70 steel in 0.5M HCl medium at 20 °C (obtained by the SIE method).....	38
Figure (III.7) :	SEM images of API 5L X70 pipeline steel in 0.5 M HCl at 20°C before and after 72 h immersion: (a) in 0.5 M HCl without inhibitor and (b) in 0.5 M HCl with 2 g/L GDE.....	40

LISTS OF TABLES

Table (II.1) :	Chemical composition of API 5L-X70 steel in mass %	23
Table (III.1) :	The values of electrochemical parameters of API 5 L X70 steel in HCl 0.5 medium at 25C°	31
Table (III.2)	Atomic percentage of various elements from the EDX analysis of the surface of API 5L X70 steel in a 0.5M HCl.....	31
Table (III.3) :	Potentiodynamic polarization parameters of API 5L X70 steel in 0.5 HCl medium containing different concentrations of GDE at 25°C.....	33
Table (III.4) :	EIS plots for API 5L X70 pipeline steel 0.5 M HCl medium with and without different concentration of GDE at 20°C.....	36
Table (III.5) :	Langmuir adsorption isotherm parameters of GDE on the surface of API 5L X70 steel in HCl 0.5 medium at 25°C.....	39
Table (III.6):	Content of elements obtained from EDX spectra for API 5L X70 pipeline steel.....	40

List of abbreviations

GDE: Ghars Date Extract

C: Inhibitor concentration

M: Molarity

θ : surface coverage

I_{corr} : corrosion current density

$I_{corr(inh)}$: corrosion current density in presence of inhibitor

b_a : cathodic coefficient

b_c : anodic coefficient

E_{corr} : corrosion potential

API: American Petroleum Institute

R_s : Resistance of solution

R_p : Resistance of polarization

R_t : Resistance of charge transfer

R'_t : Resistance of charge transfer in presence of inhibitor

Z: Impedance

Z_{imp} : Imaginary part of impedance

Z_{Re} : Real part of impedance

EIS: Electrochemical Impedance Spectroscopy

η_{SIE} : inhibition efficiency calculated from ESI

η_{pol} : inhibition efficiency calculated from potentiodynamic polarization

CPE: Constant Phase Element

C_{dl} : Double Layer Capacitance

EEC: Equivalent Electrical Circuit

ΔG_{ads}^0 : Standard adsorption free energy

K_{ads} : constant of adsorption

Z_{CPE} : the impedance of a CPE

f: frequency

T: Absolute Temperature

R: The universal constant gas

List of equation

Chapter I

$2H^+ + 2e^- \rightarrow H_2$	Eq I.1.....6
$Fe \rightarrow Fe^{+2} + 2e^-$	Eq I.2.....6
$Fe + 2H^+ \rightarrow Fe^{+2} + H_2$	Eq I.3.....6
$Fe + 3HCl \rightarrow FeCl + \frac{3}{2}H_2$	Eq I.4.....7

Chapter II

$\eta_{SIE}\% = \frac{R_t - R'_t}{R_t} \times 100$	Eq II.348
$\eta_{pol}\% = \frac{I_{corr} - I_{corr}^{(inh)}}{I_{corr}} \times 100$	Eq II.4.....50

Chapter III

$\frac{C}{\theta} = \frac{1}{K_{ads}} + C$	Eq III.4.....73
$\Delta G_{ads}^0 = -RT \ln(1 \times 10^6 K_{ads})$	Eq III.5.....73

Table of Contents

<i>Acknowledgment</i>	I
<i>List of tables</i>	II
<i>List of figures</i>	IX
<i>List of equation</i>	XII
<i>List of abbreviations</i>	XIII
General introduction	1

Chapter I: bibliographic synthesis

I.1	Corrosion of Carbon Steels in Acidic Environments	5
I.1.1	Corrosion by Concentrated Hydrochloric Acid (HCl)	5
I.1.2	Corrosion by Concentrated Sulfuric Acid (H ₂ SO ₄)	6
I.1.3	Corrosion Reactions	6
I.1.4	Potential-pH Diagram of Iron	7
I.1.5	Forms of Carbon Steel Corrosion	
I.1.5.1	Generalized Corrosion	
I.1.5.2	Pitting Corrosion	
I.1.6	Grade and Mechanical Properties of N80 Steel	7
I.1.7	Corrosion of N80 Steel	9
I.2	Protection of Carbon Steel in Acidic Environments Using Corrosion Inhibitors	9
I.2.1	Essential Properties of a Corrosion Inhibitor	10
I.2.2	Classes of Inhibitors	11
I.2.3	Synthetic and Green Inhibitors	12
I.2.4	Inhibition Mechanisms	14
I.2.4.1	<i>Adsorption Modes</i>	16
References		16

Chapter II: Study Techniques and Experimental Conditions

II.1	Study Techniques.....	31
II.1.1	Electrochemical Methods.....	31
II.1.1.1	Potentiodynamic Polarization Curves.....	31
II.1.1.2	Electrochemical Impedance Spectroscopy (EIS).....	33

II.2	Experimental Conditions.....	38
II.2.1	Working Electrodes (Materials).....	38
II.2.1.1	<i>Nomenclature</i>	39
II.2.1.2	<i>Metallographic Study</i>	40
II.2.2	Electrolyte	41
II.2.3	Corrosion Inhibitor	42
II.2.4.	Electrochemical Measurements	44
II.2.4.1	<i>Current-Potential Curves (Polarization Curves)</i>	45
II.2.5	Surface Analysis by SEM-EDX	45

References

Chapter III: Measurements and Discussions

<u>III.1 Part one</u>	Studying corrosion of API 5L X70 steel in HCl medium.....	29
III.1.1	The corrosion of API 5L X70 steel in HCl and H ₂ SO ₄ medium.....	30
III.1.2	Surface Analysis of API 5L X70 Steel in HCl Medium	31
<u>III.2 Part two</u>	Development of a Corrosion Inhibitor Treatment.....	32
III.2.1	Determination of the Optimal Inhibitor Concentration (Polarization Method).....	32
III.2.2	Impedance measurements.....	35
III.2.3	Adsorption Isotherm and Standard Free Energy of Adsorption of GDE on API 5L X70 Steel in HCl Medium	38
III.2.4	Analysis of the surface of API 5L X70 steel by SEM in HCl medium without and with the GDE inhibitor.....	39
References		41
General conclusion.....		42

General Introduction

The costs associated with corrosion in petroleum structures are very high. The economic impact—both in terms of direct and indirect losses, as well as wasted labor and financial resources—is considerable.

In recent decades, chromates (carcinogenic agents) were the most commonly used corrosion inhibitors. However, they pose significant problems due to their high potential toxicity. It is important to note that the lack of toxicity is a major weakness in many currently used inhibitory molecules. Indeed, a number of these substances are on the verge of being banned, which is why research is increasingly focused on identifying less hazardous alternatives for the environment.

Many studies have been devoted to developing organic coatings that are safe for both human health and the environment. It is certain that natural organic compounds will emerge as effective corrosion inhibitors in the coming years, due to their good biodegradability, easy availability, and non-toxic nature. A careful review of the literature clearly shows that the era of green inhibitors has already begun.

Ghars dates, obtained from Date Palm trees in Biskra (southeastern Algeria), were harvested in October 2022. The Ghars Date Extract (GDE) was naturally exuded at ambient temperature without any specific treatment or processing. This extract was chosen for the present study and employed as a corrosion inhibitor.

The work presented in this thesis focuses on studying the inhibitory effectiveness of GDE on API 5L X70 steel (pipeline grade) in acidic environments (0.5% hydrochloric acid), using surface analyses and electrochemical methods. The primary goal is to better understand the corrosion mechanism of API 5L X70 steel in acidic media and subsequently assess the inhibitory properties of the GDE inhibitor. The structure of this thesis reflects this approach.

- **Chapter I**: The first part provides a literature review on the corrosion mechanism of carbon steels in acidic environments and the influencing factors.
- **Chapter I (continued)**: The second part presents a literature review on the inhibitory properties of organic inhibitors, including influencing factors and modes of inhibition.
- **Chapter II** gives a concise overview of the experimental techniques used in this study, along with the experimental conditions adopted.

- **Chapter III** is divided into two main parts to present the results:
 - First part: Focuses on the study of API 5L X70 steel corrosion in acidic media without the presence of an inhibitor. A series of electrochemical tests and surface analyses were conducted. From the electrochemical results, the corrosion rate under various experimental conditions was determined.
 - Second part: Dedicated to optimizing the GDE concentrations for corrosion protection in acidic environments. It begins with an analysis of the mode of action of GDE.

Chapter I: Bibliographic synthesis

I.1 Corrosion of Carbon Steels in Acidic Environments

I.1.1 Corrosion by Concentrated Hydrochloric Acid (HCl)

Hydrochloric acid can be used for well acidification during oil drilling. The corrosion products formed are highly soluble in the liquid phase, which results in linear corrosion rates over time. In refineries, this acid can form at the top of the distillation column.

This acid is corrosive in its concentrated liquid form or when dissolved in an aqueous liquid phase. In its gaseous state, it is not corrosive [1].

➤ Equipment Affected by HCl Corrosion

In oil drilling, equipment used to transport and inject HCl for fracturing rocks must be resistant to this type of corrosion [1].

➤ Mechanisms and Parameters Governing HCl Corrosion

The corrosion mechanisms are electrochemical in nature, with metal oxidation as the anodic reaction and hydrogen ion reduction as the cathodic reaction. For steels, the overall reaction is:



The main parameters that govern this type of corrosion are temperature, acid concentration, and the presence of contaminants and oxidizing agents [1].

➤ Example of HCl Corrosion

Figure (I.1) shows an example of corrosion on the internal part of an aluminum bronze valve carrying concentrated hydrochloric acid [2].

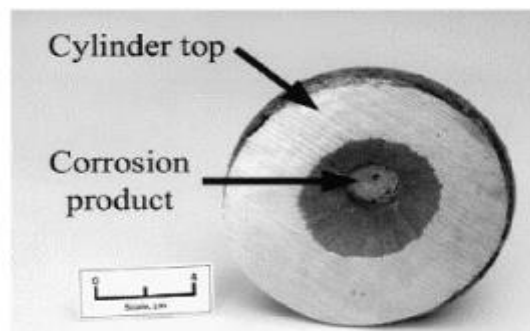


Figure (I.1): corrosion of an aluminum bronze valve by concentrated HCl [2]

I.1.2 Corrosion by Concentrated Sulfuric Acid (H₂SO₄)

Concentrated sulfuric acid is used as a catalyst in certain alkylation processes. In these units, olefins such as propylene or butylene react with isobutane to form iso-heptanes and iso-octanes. Additionally, this acid can form through the condensation of sulfurous fumes.

It can also be present in wastewater treatment units. This acid is generally corrosive in its concentrated liquid state (under certain conditions, it can passivate steels) or when dissolved in an aqueous liquid phase. In its gaseous state, it is not corrosive [1].

➤ Equipment Affected by H₂SO₄ Corrosion

In alkylation units, the affected equipment includes:

- Storage tanks for fresh and spent sulfuric acid [3, 4]
- Effluent lines from reactors
- Reboilers
- Caustic wash reactors
- Overhead sections of depropanizer columns

At the outlet of towers, sulfuric acid can form in fumes through the reaction of SO₂ and SO₃ with water vapor, according to the following reactions [1]:



(Occurs in the gaseous state below 200°C)

➤ Mechanisms and Parameters Governing H₂SO₄ Corrosion

The corrosion mechanisms are electrochemical, with metal oxidation as the anodic reaction and ion reduction as the cathodic reaction. For steels, the overall reaction leads to iron dissolution and the formation of iron sulfate as follows:



Corrosion takes a generalized form when the acid covers the entire metallic surface, or a localized form when acid droplets condense in specific areas.

The main parameters that govern this corrosion are temperature, acid concentration, hydrodynamic flow velocity, and the presence of contaminants and oxidizing agents.

An increase in temperature up to the vaporization point results in an increase in corrosion. For alloys that are protected by the formation of a protective metal sulfate layer, excessively high flow rates can strip this layer, leading to significant corrosion rates.

The presence of contaminants such as chlorine, and oxidizing agents such as O_2 , Fe^{3+} , and Cu^{2+} in the liquid sulfuric acid accelerates corrosion [1].

➤ Example of Corrosion by H_2SO_4

A carbon steel furnace tube in a boiler experienced generalized corrosion during a unit shutdown (Figure 1.2). This furnace was heated by a heavy crude oil rich in sulfur. During the shutdown, SO_3 compounds reacted with atmospheric water vapor, thereby forming sulfuric acid.

To prevent this type of corrosion, neutralization by injecting ammonia or carbonated water would have been necessary [1].



Figure (1.2): Example of corrosion by H_2SO_4

I.1.3 Corrosion Reactions

The corrosion of metals is due to an irreversible redox (oxidation-reduction) reaction between the metal and an oxidizing agent present in the environment. The oxidation of the metal involves the reduction of the oxidizing agent:



For example, the corrosion of iron in hydrochloric acid (Figure 3) results from reaction (1.1):

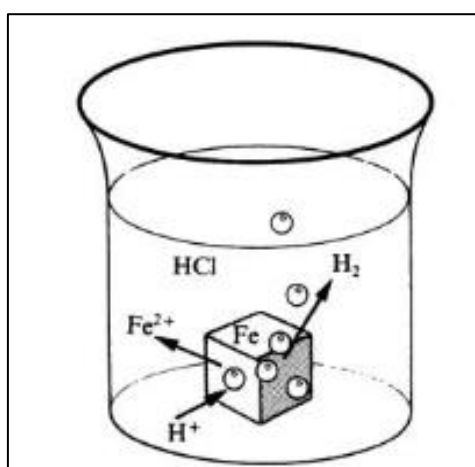
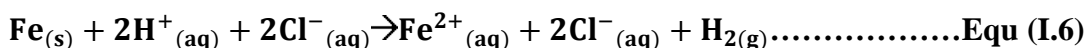


Figure (I.3) : iron corrosion in an acidic environment

In this equation, the subscripts (s), (aq), and (g) refer to the solid, aqueous, and gaseous phases, respectively. In an aqueous medium, hydrochloric acid and ferrous chloride are in ionic form. Thus, the reaction can also be written as:



Here, the oxidizing agent is the solvated proton H⁺(aq). The reaction products are the solvated ferrous ion Fe²⁺(aq) and hydrogen gas H₂(g). For simplicity, phase indicators are usually omitted. Furthermore, since chloride ions do not directly participate in the reaction, equation (I.6) can be simplified as:



For this reason, we distinguish **wet corrosion**, or corrosion at ambient temperature [5].

➤ Partial Reactions

Every redox (oxidation-reduction) reaction consists of two half-reactions:

- **Anodic half-reaction** (oxidation), and
- **Cathodic half-reaction** (reduction).

For example, in the corrosion of iron:



The anodic and cathodic half-reactions explicitly show the electrons exchanged during the redox process, which is not visible in the overall reaction. Electrochemical Reaction is a chemical transformation that involves charge transfer at the interface between: an electronic conductor (called the electrode) and an ionic conductor (called the electrolyte).

An electrochemical reaction may include one or more electrode reactions. For example, reaction (1.7) is an electrochemical reaction: Each iron atom entering solution exchanges two electrons with protons. Thus, it includes two electrode reactions: Oxidation of iron, and Reduction of protons. According to the above definition, all corrosion reactions that involve oxidation of the metal are electrochemical reactions [5].

1.1.4 Potential-pH Diagram of Iron

Given the importance of steels in engineering construction, understanding the corrosion behavior of iron is critical. Figure 1.3 shows the potential–pH diagram (Pourbaix diagram) for iron. It considers the stability of two iron oxides:

- **Hydrated Fe₂O₃**
- **Fe₃O₄ (magnetite)**

The concentration of dissolved species is taken as 10^{-6} mol/L. From this diagram, one can observe:

[Chapter I: Bibliographic synthesis]

- In acidic and neutral environments, iron reacts with protons, releasing hydrogen gas.
- In alkaline environments, iron resists corrosion because the oxides formed are insoluble and do not react easily with hydroxide ions.

This behavior aligns with practical observations; in acidic or neutral environments, unprotected steel corrodes easily. In alkaline environments, such as concrete, it exhibits good corrosion resistance [5].

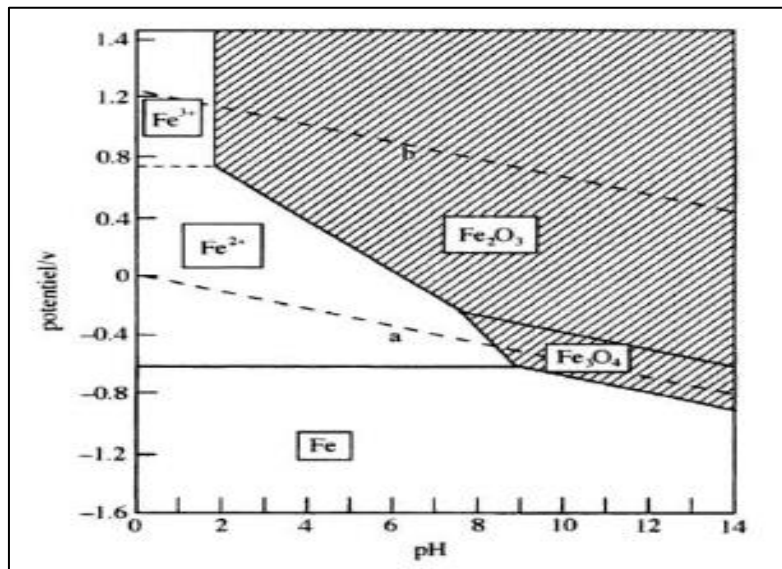


Figure (1.4): Iron potential-pH diagram (T=25°C). The concentration of the dissolved ionic species $C_{Fe^{3+}}$ and $C_{Fe^{2+}}$ worth 10^{-6} mol/L

According to the diagram in Figure I.3, iron can exist in three thermodynamic states depending on its potential and the pH of the solution in which it is immersed:

- **Passivation:**
A protective zone where the metal is shielded by the formation of oxides or hydroxides on its surface (Fe_2O_3 , Fe_3O_4);
- **Corrosion:**
A zone where the metal is attacked with the formation of ions (Fe^{3+} , Fe^{2+}). Corrosion may occur in both acidic and basic environments;
- **Immunity:**
A zone where metallic iron (Fe) is thermodynamically stable.

1.1.5 Forms of Carbon Steel Corrosion

Corrosion affects metals in various ways, depending on their nature and the environmental conditions. There is a broad classification of different forms of corrosion, among which two main types have been identified.

1.1.5.1 Generalized Corrosion

This type of corrosion is characterized by an attack over the entire surface of the exposed metal sample [6]. It is commonly observed in metals exposed to acidic environments [7].

This phenomenon is defined by the rate of attack, which can be measured either in millimeters per year or in milligrams per square decimeter per day [7]. In this mode of corrosion, at a macroscopic scale, cathodic and anodic sites are indistinguishable [7].

Generalized corrosion is the most widespread form and can often be detected long before it causes significant damage to the structural integrity of the metal. Factors such as flow velocity, pH, and temperature of the environment have a significant influence on the uniform corrosion rate (Figure 1.5) [7].

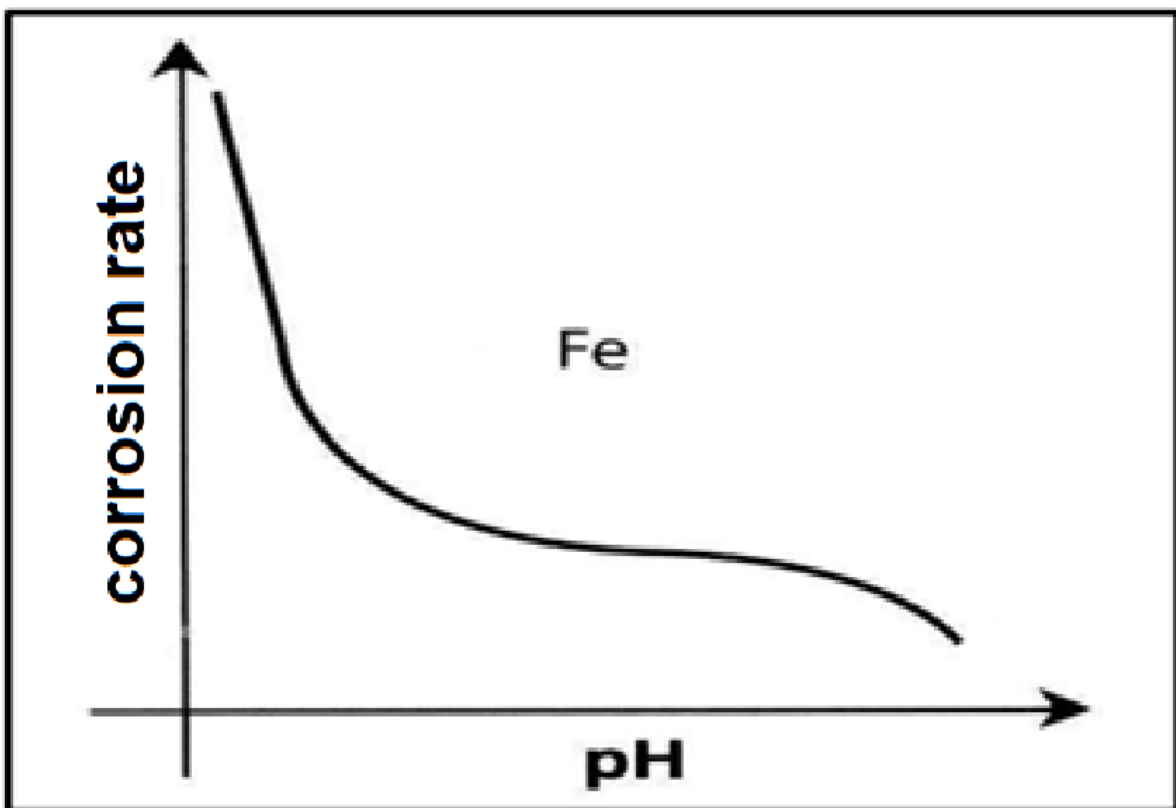


Figure (1.5): Variation of corrosion rate with pH [7]

1.1.5.2 Pitting Corrosion;

It occurs when metals protected by a thin oxide film, such as aluminum and its alloys or stainless steels, come into contact with an aqueous environment (with a pH close to neutral) containing halides, particularly chloride ions (Cl^-). The amount of metal that corrodes is very small, yet it creates cavities a few tens of micrometers in diameter inside the material, starting from a small surface opening.

The pitting corrosion process involves two stages:

- 1) Initiation, which occurs when the passive film is locally broken.
- 2) Growth or propagation of the pit. [9–11]

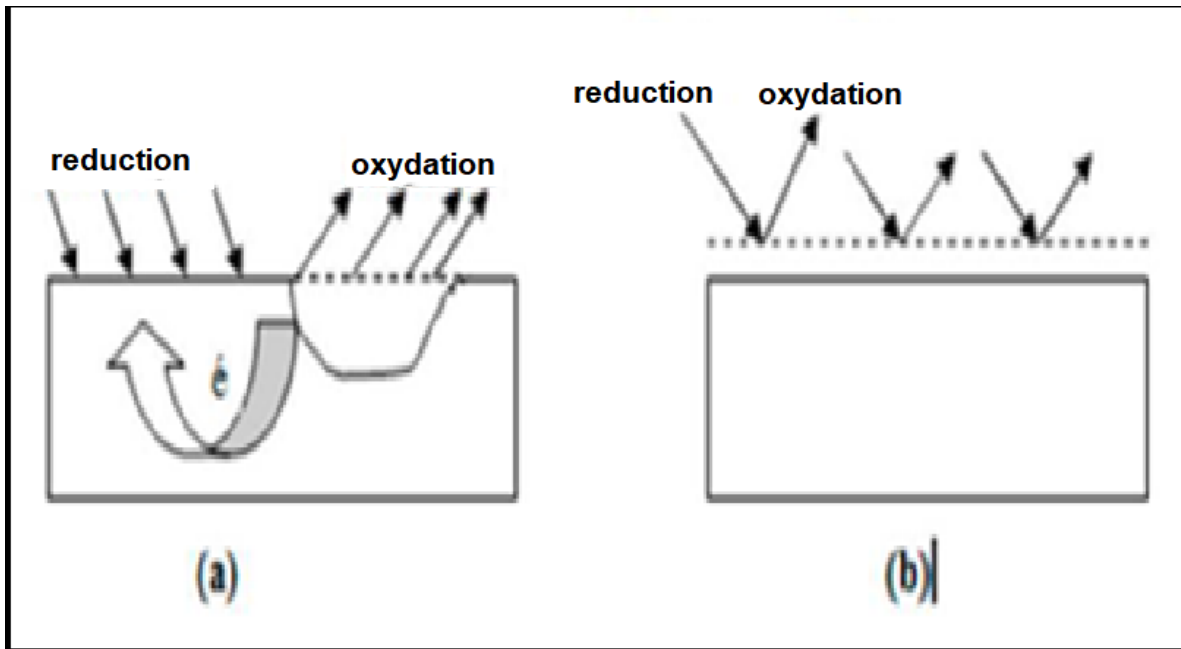


Figure (1.6): (a) Localized corrosion (b) Homogeneous corrosion of a metal [8]



Figure (I.7) Pitting Corrosion of inox-steel

I.1.6 Grade and Mechanical Properties of N80 Steel

The specific grade of the steel used in available tubing is generally unknown. Since the N80 grade, which is the lowest standard specified by API, corresponds to a yield strength of 550 MPa, we know that these tubes have at least this minimum yield strength. In most cases, this value is used as a reference without carrying out sampling for further characterization.

The joining (raboutage) of these tubes involves various designs depending on their application (tubing or casing). Some types of joints, though bulky, guarantee a resistance—regardless of the type of stress applied—that is greater than that of the straight sections.

It is not advisable to perform just any type of welding under field conditions on petroleum tubing. Generally, it is acceptable to attach accessories using non-structural tack welds, but rejoining (raboutage) should only be done in a workshop with an appropriate choice of filler metal, and procedures for fabrication and inspection suited to the intended purpose [12].

I.1.7 Corrosion of N80 Steel

➤ Chemical (Dry) Corrosion:

Chemical corrosion is the direct attack of the metal by its environment. This type of corrosion occurs in non-electrolyte solutions or from the action of gases (such as O₂, H₂S, and CO₂). When the reactive agent is gaseous or when this corrosion occurs at high temperatures, it is called dry corrosion or high-temperature corrosion [13, 14].

➤ Electrochemical (Wet) Corrosion:

When the corrosive agent is liquid, the process generally involves electrochemical corrosion, primarily caused by the oxidation of a metal into ions or oxides and the simultaneous reduction of corrosive agents present in the electrolytic solution.

This type of corrosion results from electron transfer between the metal and the electrolyte in contact with it (creating an electrical current). The presence of heterogeneities, whether in the metal or the environment, causes the formation of a galvanic cell, allowing electric current to flow between anodes and cathodes within the medium, and the zones acting as anodes are corroded.

This corrosion requires the presence of a reductant (e.g., H₂O, H₂). Without it, metal corrosion (anodic reaction) cannot occur [15, 13, 14].

I.2 Protection of Carbon Steel in Acidic Environments Using Corrosion Inhibitors

Corrosion inhibitors are a unique approach to combatting metal corrosion. What makes them distinctive is that they are not applied directly to the metal, but rather added to the corrosive environment. According to ISO 8044, an inhibitor is defined as:

"A chemical substance added to a corrosion system at a concentration chosen for its effectiveness; this results in a decrease in the corrosion rate of the metal without significantly altering the concentration of any corrosive agent present in the aggressive medium." [16]

The National Association of Corrosion Engineers (NACE) defines an inhibitor as:

"A substance that retards corrosion when added in small amounts to an environment." [17]

I.2.1 Essential Properties of a Corrosion Inhibitor

Generally, a corrosion inhibitor should:

- ✓ Reduce the corrosion rate of a metal without altering its physical-chemical properties, especially mechanical strength (e.g., avoid hydrogen embrittlement in acidic media);
- ✓ Remain stable in the presence of other environmental components, particularly oxidizing agents;
- ✓ Be thermally stable at operating temperatures;
- ✓ Be effective at low concentrations;
- ✓ Be compliant with non-toxicity standards;

- ✓ Be cost-effective [18].

I.2.2 Classes of Inhibitors

Corrosion inhibitors can be classified in several ways, notably:

- By product formulation: organic or inorganic inhibitors;
- By electrochemical mechanism of action: cathodic, anodic, or mixed inhibitors;
- By interface mechanisms and principles of action: through adsorption and/or film formation [19, 5]

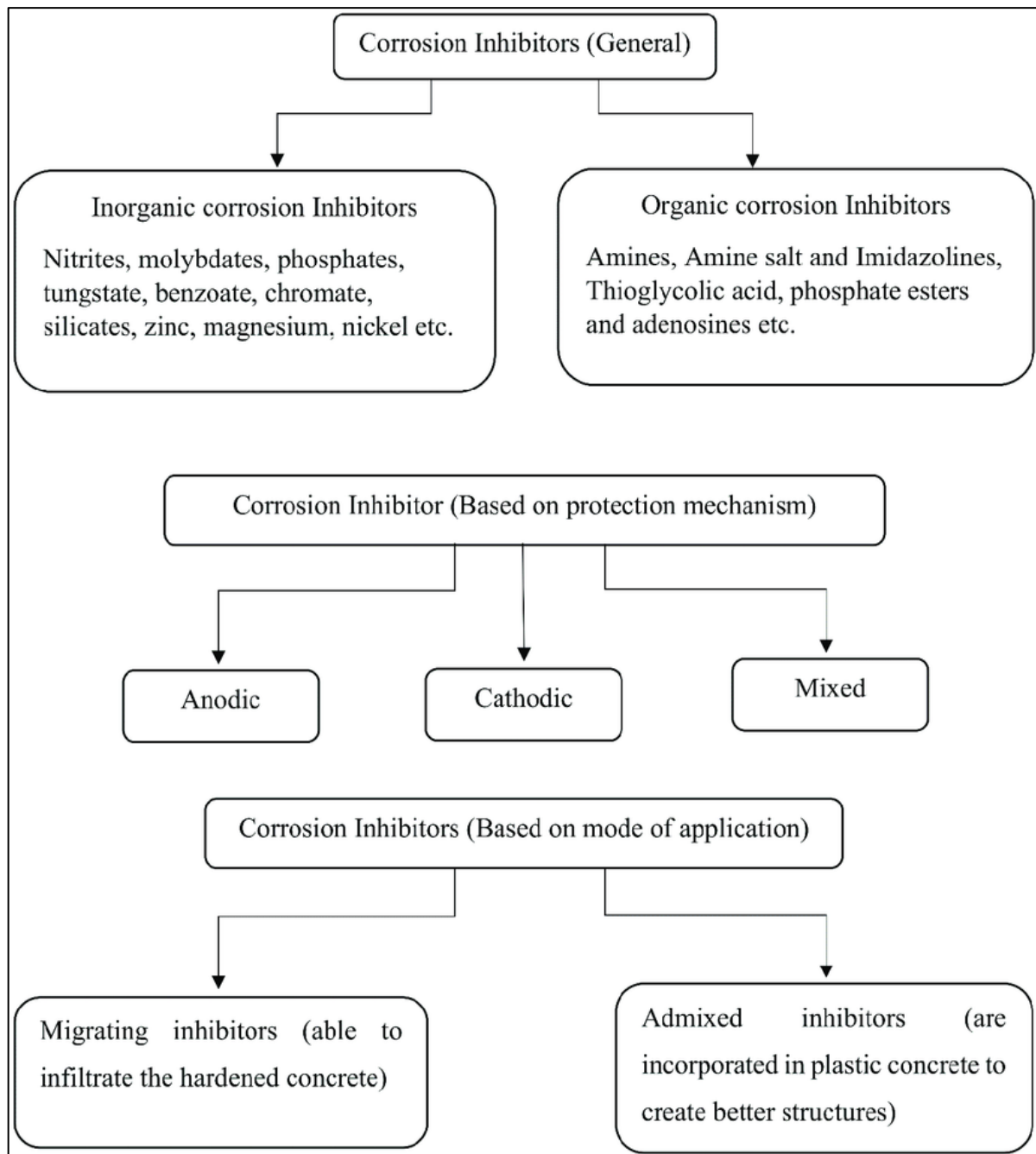


Figure (I.8): Classes of Inhibitors

I.2.3 Synthetic and Green Inhibitors

Organic molecules are poised for significant development as corrosion inhibitors: their use is now preferred over inorganic inhibitors due to concerns about ecotoxicity. Organic inhibitors can be divided into two categories:

- Natural organic inhibitors

- Synthetic organic inhibitors (most are non-biodegradable and costly)

As a result, natural organic inhibitors are increasingly favored. A thorough review of the literature clearly shows that natural polymers are the best choice for protecting carbon steel in acidic environments.

I.2.4 Inhibition Mechanisms

The various reactions between material and electrolyte can be inhibited in several ways, with the most important being:

- **Adsorption:**

Adsorption of the inhibitor onto the metal surface can slow corrosion. In this case, the inhibition efficiency depends primarily on the molecular structure and concentration of the inhibitor.

- **Passivation:**

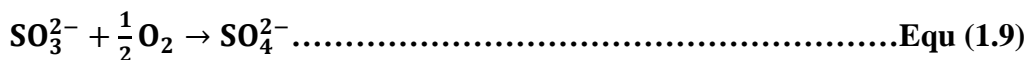
Some oxidizing inhibitors induce spontaneous passivation of the metal, which reduces the corrosion rate.

- **Precipitation:**

Other inhibitors promote the formation of surface films via precipitation of mineral salts or low-solubility organic complexes. These films reduce the surface's exposure to oxygen and also partially block anodic dissolution.

- **Removal of the corrosive agent:**

This inhibition mechanism is only applicable in closed systems. It involves adding a small quantity of sodium sulfite or hydrazine to pre-degassed and deionized water, which removes the remaining traces of oxygen and eliminates corrosion according to the following reactions [10]:



I.2.4.1 Adsorption Modes

Adsorption is a universal surface phenomenon, as all surfaces are made up of atoms with unsatisfied chemical bonds. These atoms tend to fulfill these missing bonds by capturing nearby atoms or molecules. Two types of adsorptions are distinguished:

- **Physisorption** (physical adsorption):

This maintains the identity of the adsorbed molecules and involves weak interactions.

There are three main types of forces:

- ❖ Dispersion forces (Van der Waals, London), always present;
- ❖ Polar forces, resulting from electric fields;
- ❖ Hydrogen bonding, typically involving hydroxyl or amine groups.

- **Chemisorption** (chemical adsorption):

This involves the sharing of electrons between the polar part of the molecule and the metal surface, leading to the formation of strong chemical bonds with higher bond energies. The electrons primarily come from lone electron pairs on atoms such as O, N, S, P—all of which are highly electronegative.

Chemisorption results in a significant redistribution of electronic charges in the adsorbed molecules and is often an irreversible process [20].

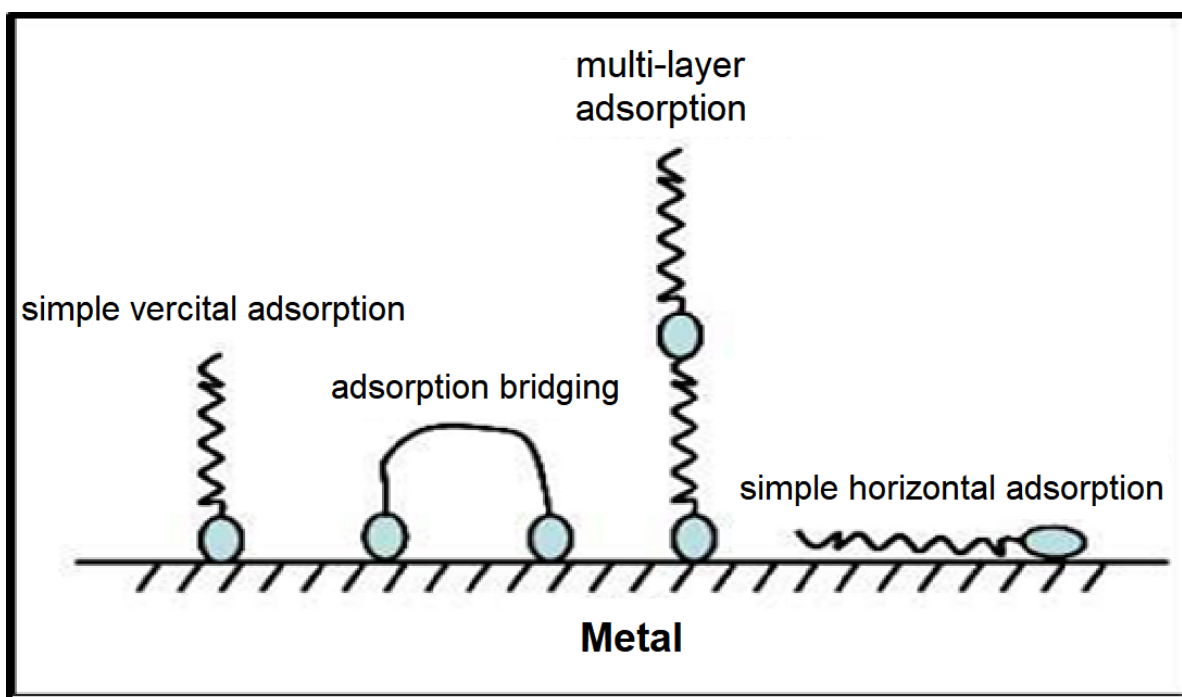


Figure (I.9) Adsorption Modes

References

1. R. François, *Corrosion et dégradation des matériaux métalliques: Compréhension des phénomènes et applications dans l'industrie pétrolière et des procédés*, Éd. Technip, 2009.
2. H. GR, *Failure analysis of an HCL*, *Engineering Failure Analysis*, 6,7 (2000) 403-409.
3. *Materials of Construction for Handling Sulfuric Acid*, NACE (1985).
4. NACE, *recommended practice for the design , fabrication , and inspection of tanks for the storage of petroleum refining alkylation unit spent sulfuric acid at ambient temperature* NACE RP 0205, (2005).
5. D. Landolt, *Corrosion et chimie de surfaces des métaux*, Presses polytechniques et universitaires romandes, 1997.
6. V.Q.kinth, *Corrosion et protections des matériaux métalliques*, callaquechimie, (2008).
7. A.D. B.Schramm, A.Kuhlles, *revêtement et lacorrosion*, *Technique compact* 10e édition, (décembre2004).
8. M. khalida, *Contribution à l'étude de l'incompatibilité entre un inhibiteur de corrosion et un inhibiteur de dépôt*, in, m'hamed boumerdes, 2014.
9. *Matériaux Métalliques "Phénomènes de Corrosion, 4ième partie " Les différentes formes de corrosion aqueuse"*.
10. H.E. bakouri, *Etude de l'inhibition de la corrosion de l'acier doux au carbone en milieu acide orthophosphorique par un antibiotique organique*, in, Université Mohammed I, oujde.
11. S. KHIRECHE, *Elaboration et étude de la corrosion des alliages Al-Zn et Al-Sn dans une solution à 3% en poids NaCl*, in, Tizi ouzou.

12. P.n. FOREVER, *Forever: synthèse des résultats et recommandations du projet national sur les micropieux*, Presses de l'École nationale des ponts et chaussées, 2004.
13. R. Mehibil, *Etude de l'efficacité inhibitrice de quelques nouveaux inhibiteurs, dits non polluants, sur la corrosion de deux types d'alliages d'aluminium*, in, skikda, skikda, 2008.
14. D.N.R. Rabah, *introduction à la corrosion et aux inhibiteurs de corrosion.*, 2004.
15. S. BENSAADA, *corrosion*, biskra, 2010.
16. V.C. G. Trabanelli, *Corrosion Science and Technology*, Plenum Press, (1972).
17. S. Bradford, *Corrosion and Protection*, New York, 1992.
18. M. Lebrini, *Etude de la tenue à la corrosion de l'acier N80 et évaluation de l'efficacité d'un inhibiteur de corrosion*, in, Université des sciences et technologies, lille, 2005.
19. C.L. C. Fiaud, N. Pébère, *Corrosion et anticorrosion*, 2002.
20. JeanSarrazinetMichelVerdaguer, *L'oxydoréduction*, Edition Ellipses, 1997.

Chapter II: Study technique and experimental conditions

II.1 Study Techniques

To study corrosion phenomena in different corrosive environments and the properties of inhibitors, three types of methods were used:

- **Electrochemical methods (polarization curves):** These provide a better understanding of the corrosion mechanism in different corrosive environments and help evaluate the efficiency and mechanism of action of the studied inhibitor.
- **Immersion methods (weight loss):** These were used to determine the corrosion rate with and without the inhibitor.
- **Surface analyses (optical microscopy):** These were employed to determine the condition of the working electrode and the nature of the layer that forms on its surface, thereby confirming the effectiveness of the studied inhibitor.

II.1.1 Electrochemical Techniques

Electrochemical methods are based on the characterization of redox reactions involving electron exchange between the oxidant and the reductant. These measurements characterize modifications at the metal/environment interface. Polarization curve plotting provides quantitative data, giving values of physical parameters describing the system's state (corrosion current, inhibition rate, polarization resistance).

II.1.1.1 Polarization Curves

An electrochemical reaction on an electrode is governed by the applied overpotential, which is the difference between the electrode/solution potential and the equilibrium potential of the reaction. The current intensity through the material is a function of the potential, represented by a curve that is the sum of the currents from the electrochemical reactions at the electrode surface. Its determination in a corrosive environment allows the study of corrosion phenomena.

Polarization curves are determined by applying a potential between a working electrode and a reference electrode. A steady-state current establishes after a certain time (minutes to hours). This current is measured between the working electrode and a counter (auxiliary) electrode.

[Chapter II: Study technique and experimental conditions]

From a kinetics point of view, two control modes are distinguished based on the rate-limiting step [1]:

- Charge transfer at the metal/electrolyte interface (activation),
- Mass transport of the electroactive species or reaction products.

Polarization curves of activation-controlled reactions follow the Butler-Volmer equation [2]:

$$i = i_0 \exp\left(\frac{\eta}{b_a}\right) - i_0 \exp\left(-\frac{\eta}{b_c}\right) \dots\dots\dots \text{Equ (II.1)}$$

Where:

- i is the current density,
- i_0 the exchange current density,
- η , eta the electrode overpotential ($E - E_{\text{corr}}$).

When plotted on a logarithmic scale, the curves exhibit, far from equilibrium, two linear branches called Tafel lines, indicating that the reaction associated with the applied polarization dominates. The slopes of these lines (Tafel coefficients β_a and β_c) and the exchange current density i_0 , linked to the rates of the anodic and cathodic partial reactions at equilibrium, reflect the reaction mechanism and the metal's dissolution rate.

Diffusion-controlled reactions follow Tafel's law at low overpotentials but exhibit current saturation at high overpotentials, where diffusion becomes the limiting factor. The diffusion flux of this species at the electrode/solution interface then determines the reaction rate and thus the current intensity [3].

II.2 Experimental Conditions

II.2.1 Working Electrodes

II.2.1.1 Nomenclature

Steel grade designation is a conventional system to name, identify, or classify steels. These are established by organizations involved in standardization, such as the European Committee for Standardization (CEN), the International Organization for Standardization

[Chapter II: Study technique and experimental conditions]

(ISO), or professional certification bodies like the American Iron and Steel Institute (AISI) or the American Petroleum Institute (API).

Carbon steel is defined as steel where carbon is the principal alloying element, ranging from 0.12% to 2.0%, and other alloying elements are present in very small amounts.

According to AISI, a steel is considered carbon steel when no minimum content is specified or required for elements like chromium (Cr), cobalt (Co), niobium (Nb), molybdenum (Mo), nickel (Ni), titanium (Ti), tungsten (W), vanadium (V), or zirconium (Zr), and the maximum permitted content for elements like [4]:

- Manganese (Mn): 1.65%
- Silicon (Si): 0.60%
- Copper (Cu): 0.60%

Note that designations vary across countries; AISI, AFNOR, API, CEN, and ISO are not the only standards.

The material used as the working electrode is carbon steel API 5L X70, with its chemical composition listed in Table II.1. API 5L X70 is a carbon steel designated by its yield strength:

- API 5L: Indicates pipeline-grade steel.
- X70: Indicates grade (others include A, B, X42, X60).
- 70: Refers to 70,000 psi (pounds per square inch) yield strength.

Table II.1: chemical composition of API 5L X70 carbon steel in mass % [5].

C (max)	Mn (max)	Si (min)	P (max)	S (max)	Cu (max)	Ni (max)	Nb (max)	V (max)	Mo (max)
0,140	1,700	0,150	0,020	0,005	0,080	0,250	0,040	0,080	0,250

II.2.1.2 Metallographic Study

To determine the metallographic structure of API 5L X70 steel, a sample was polished on SiC abrasive discs of various grit sizes (P120 to P1200), rinsed with distilled water, and dried with paper tissue. A metallographic etch was performed by immersing the polished steel in 2% nital (2% nitric acid in ethanol) for 20 seconds.

Optical microscopy revealed that the steel has a ferrite-pearlite microstructure (Figure II.1).

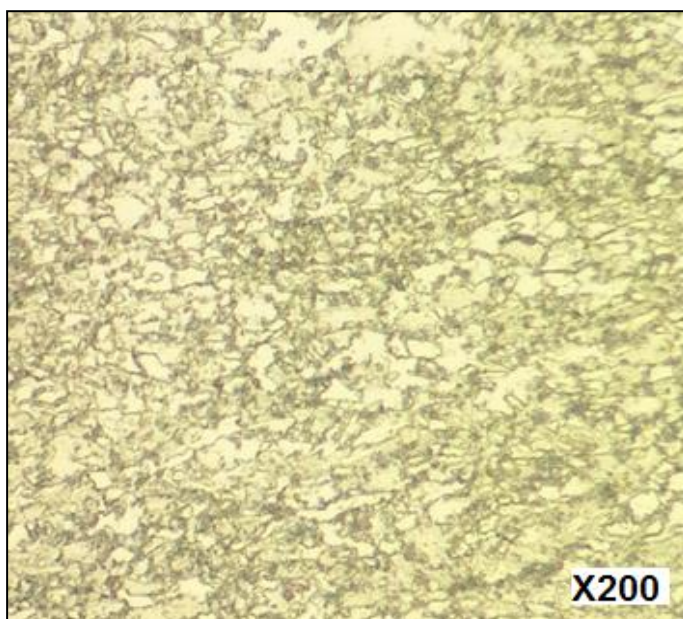


Figure (II.1): Metallographic structure of API 5L X70 carbon steel produced after 2% nital attack.

II.2.2 Electrolyte

For industrial relevance, the chosen electrolyte was an aqueous solution of hydrochloric acid (0.5 M). Aggressive HCl solutions were prepared by diluting 37% HCl with distilled water.

II.2.3 Corrosion Inhibitor

Ghars dates, obtained from Date Palm trees in Biskra (southeastern Algeria), were harvested in October 2022. The Ghars Date Extract (GDE) was naturally exuded at ambient temperature without any specific treatment or processing. This extract was chosen for the present study and employed as a corrosion inhibitor. Galacturonic acid, a major constituent of

[Chapter II: Study technique and experimental conditions]

the polysaccharides present in date palm fruits, represents a key component of the extract. The molecular structure of galacturonic acid is illustrated in Figure II.2 [6].

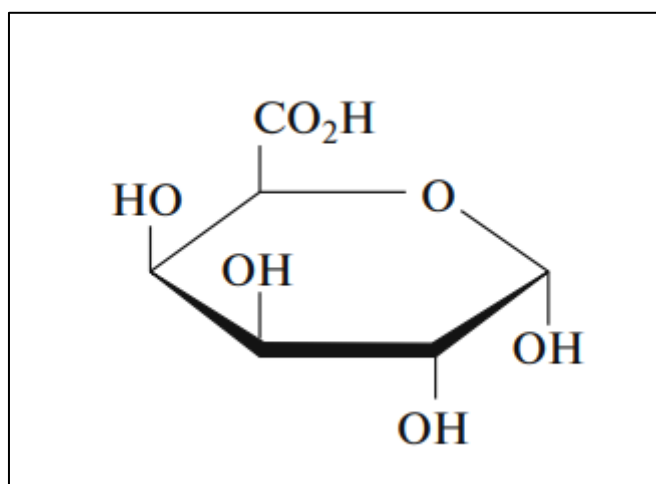


Figure II.2: The molecular structure of galacturonic acid

II.2.4 Electrochemical Measurements

Electrochemical tests were carried out using a potentiostat/galvanostat 3000 with Gamry Instruments software, in a three-electrode plexiglass cell:

- A working electrode (API 5L X70 steel),
- A saturated calomel reference electrode (Ag/AgCl), placed close to the working electrode to minimize ohmic drop,
- A chemically inert counter electrode (graphite).

Before each test, the cell was cleaned with ethanol, rinsed with distilled water, and dried with absorbent paper. The system was connected to a computer. Before measurements, the working electrode was immersed in the test solution at open circuit potential for 30 minutes to reach a stable state. A thermostatic bath was used to maintain the solution at the desired temperature (Figure II.3).

For plotting curves, processing, and analyzing the electrochemical measurements, all data were transferred from Voltmaster 4 to Origin 9.0 (a scientific data analysis software).

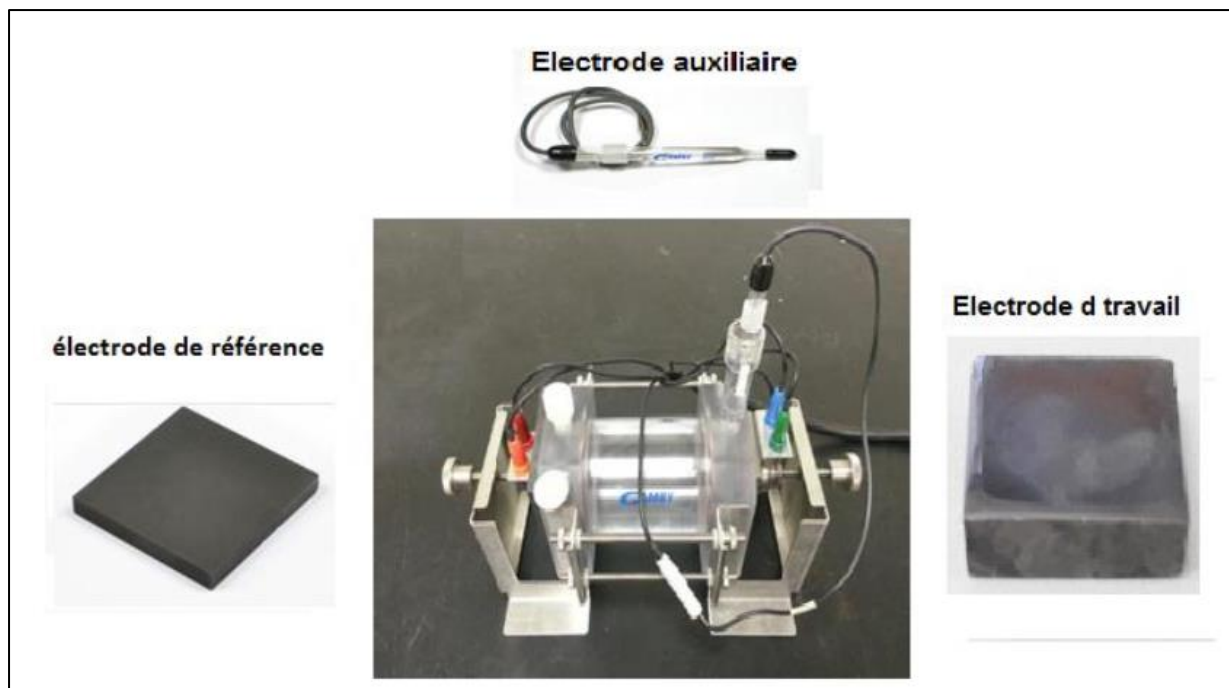


Figure II.3: Photograph of the electrochemical measuring device

II.2.4.1 Current-Potential Curves (Polarization Curves)

We used the Tafel method to determine the corrosion rate (graphical method), particularly when the Tafel slopes showed significant non-linearity. The inhibition efficiency (η_{pol}) was calculated using the following equation:

$$\eta_{POL} \% = \frac{I_{corr} - I_{corr(inh)}}{I_{corr}} \times 100 \dots\dots\dots \text{Equ II.2}$$

Where I_{corr} and $I_{corr(inh)}$ represent the corrosion current densities without and with the inhibitor (GDE), respectively.

II.2.5 Surface Analysis by SEM-EDX

To examine the surface morphology changes of API5L X70 steel, the samples were immersed in a 0.5 M sulfuric acid solution containing the optimal concentration of the inhibitor (Ghars Date Extract). After 96 hours of immersion, the samples were removed and dried. A scanning electron microscope, TESCAN VEGA3, from the LPCMA laboratory at the University of Biskra, was used for the SEM-EDX analysis.

References

1. R.F. A.J. Bard, *Electrochimie – Principes, méthodes et applications*, Paris, 1983.
2. D. Landolt, *Corrosion et chimie de surfaces des métaux*, Presses polytechniques et universitaires romandes, 1997.
3. P. Sandrine, *Comportement à la corrosion galvanique de matériaux composites à matrice d'alliage d'aluminium renforcée par des fibres de carbone haut-module*, in, UNIVERSITÉ BORDEAUX I, Doctorat 2001.
4. C.L. C. Fiaud, N.Pebere, *Inhibiteurs de corrosion*, Lavoisier ed., Hermès Science Publications 2002.
5. A.T.d. Annaba, in: *O.d.e.f.e.c. Département assurance qualité (Ed.)*, 2012.
6. Freitas, C.M.P., R.C.S. Sousa, M.M.S. Dias, and J.S.R. Coimbra, *Extraction of Pectin from Passion Fruit Peel*. *Food Engineering Reviews*, 2020. **12**: p. 460 - 472.

Chapter III: Results and Discussion

Part I

III.1 Study of the Corrosion Kinetics of API 5L-X70 Steel in 0.5 M HCl Medium

This section is dedicated to evaluating the corrosion behavior of API 5L X70 steel in a 0.5 M HCl solution. For this purpose, a series of electrochemical tests and surface analyses were carried out. From the electrochemical tests, the corrosion rate was determined.

III.1.1 Polarization Curve of API 5L-X70 Steel

The polarization curves of API 5L X70 steel exhibit two potential domains (Figure

- **Active Domain (Zone I):**

Located between E_{corr} and E_{pit} , in this domain there is active dissolution of the steel according to the reaction:



The electrons released by the active dissolution are consumed by protons in the medium to form hydrogen gas molecules according to the reaction:



The corrosion kinetics are entirely governed by charge transfer reactions.

- **Zone II:**

This is the pitting corrosion zone. Beyond E_{pit} , the current density increases rapidly. The absence of a passive layer was observed due to the presence of aggressive anions.

Table III-1 presents the electrochemical parameters determined from the polarization curves of API 5L X70 steel in 0.5 M HCl medium.

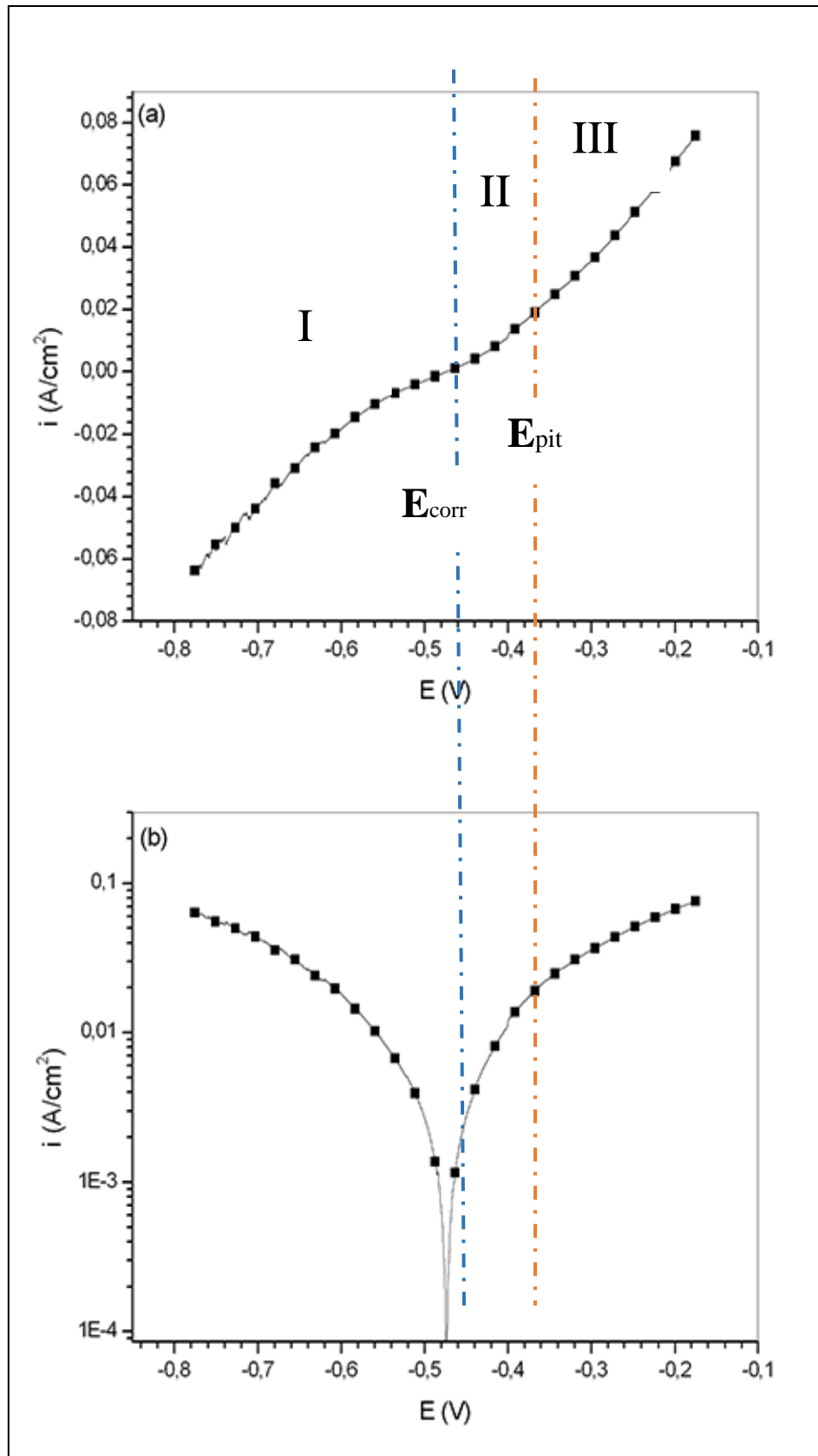


Figure III.1: Polarization curves of API 5 L X70 steel in 0.5 M HCl medium at 25°C, (a) linear curve, (b) logarithmic curve.

Chapter III: Measurements and Discussions

Table (III.1): Values of electrochemical parameters of API 5 L X70 steel in 0.5M HCl medium at 25C°.

Medium	E_{corr} (mVvs.SCE)	I_{corr} ($\mu\text{A}/\text{cm}^2$)	E_{pit} (mVvs.SC E)	-bc (mV/dec)	ba (mV/dec)
HCl 0.5	-472	755	-400	128	100

III.1.2 Surface Analysis of API 5L X70 Steel in HCl Medium

To determine the nature of the corrosion products formed on the steel surface, samples were immersed in a 0.5 M HCl solution bath for 24 hours.

Figure (III.2) shows the macroscopic appearance of the corrosion products on the steel surface.

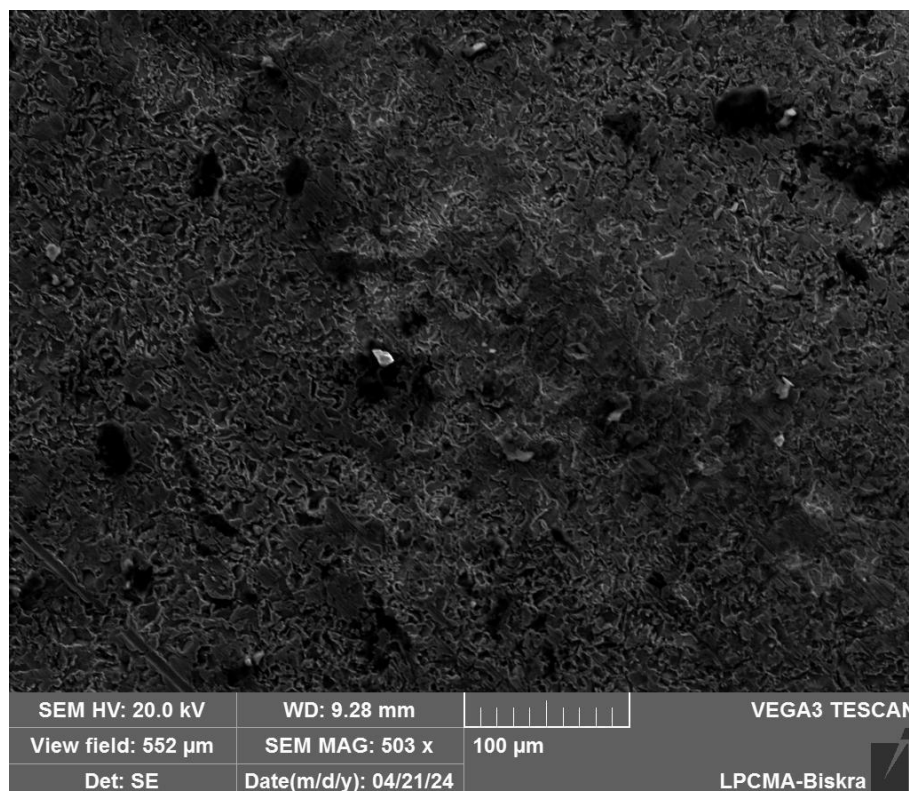


Figure III.2: Morphology of corrosion of API 5L X70 steel observed by SEM in HCl environments (immersion time: 72 hours).

Table III.2: Atomic percentage of various elements from the EDX analysis of the surface of API 5L X70 steel in a 0.5M HCl

Element	% atomic of X70	% atomic X70 +HCl
Fe	97.12	60
O	2.88	37
Cl	-	2.00

Part II

III.2 Development of a Corrosion Inhibitor Treatment

This section focuses on evaluating a corrosion treatment for API 5L X70 steel in 0.5 M HCl medium.

The concentrations of the inhibitor were optimized to obtain a cost-effective inhibitor that can provide good protection against corrosion in 0.5 M HCl medium. Additionally, the adsorption isotherm was studied.

III.2.1 Determination of the Optimal Inhibitor Concentration (Polarization Method)

The linear and logarithmic polarization curves of API 5L X70 steel in HCl at 25°C, in the absence and presence of GDE at different concentrations, are shown in Figure (3.4).

The corrosion potential values shift slightly. Generally, if the E_{corr} shift exceeds 85 mV compared to the uninhibited solution, the inhibitor type can be considered anodic or cathodic [1, 2]. In our study, the maximum shift was 30 mV, indicating that GDE acts as a mixed-type inhibitor.

The partial anodic and cathodic current densities decreased, meaning a reduction in the corrosion rate. This shift of the anodic and cathodic branches to lower values is a result of the inhibition of the anodic and cathodic reactions of API 5L X70 steel by GDE.

The Tafel anodic and cathodic lines are not parallel, likely not because of GDE itself, but due to corrosion products that may influence the mass transport mechanism during steel dissolution, which is controlled by charge transfer.

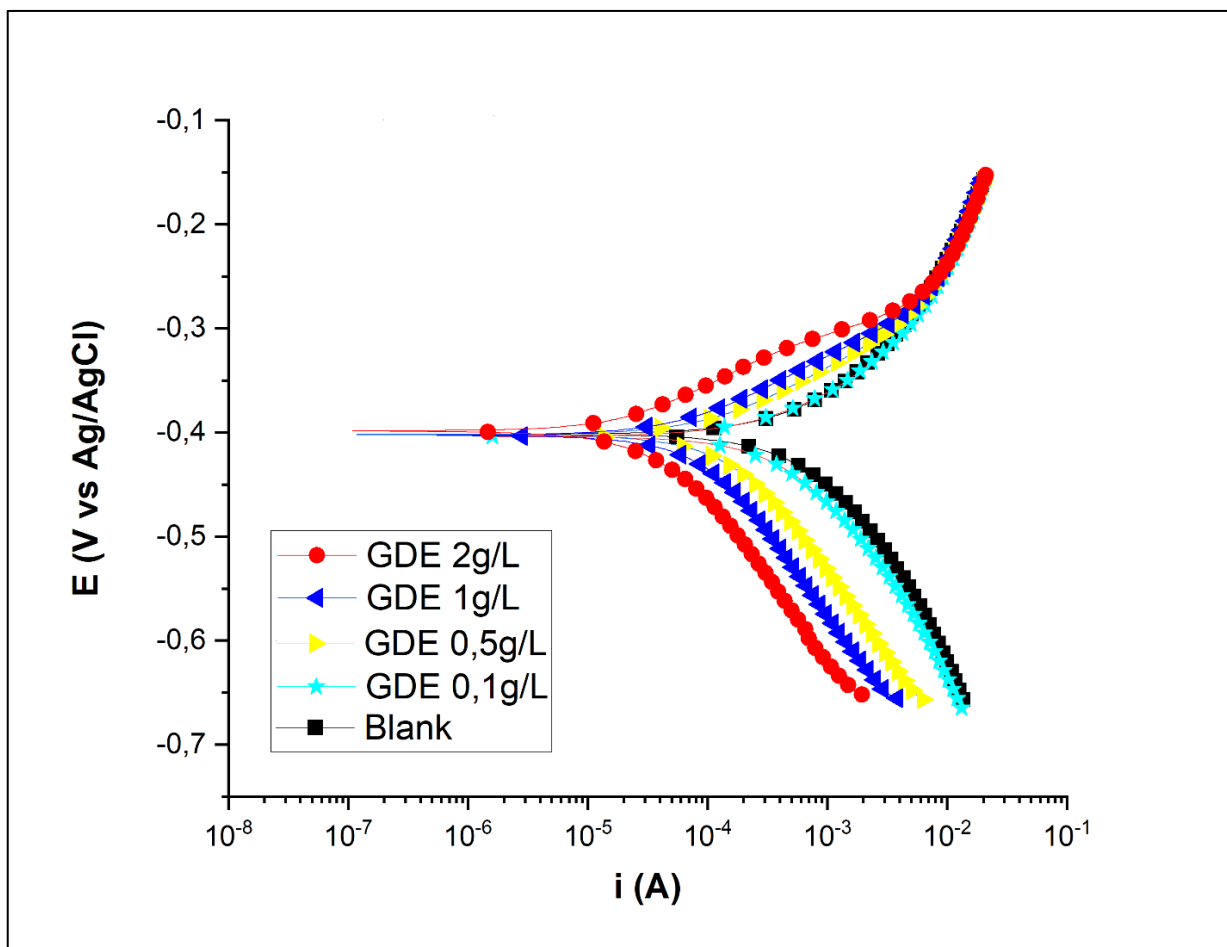


Figure III.3: Potentiodynamic polarization curves for API 5L X70 pipeline steel in 0.5 M HCl without and with different concentrations of GDE at 20°C.

Table III.3: Potentiodynamic polarization parameters for API 5L X70 pipeline steel in 0.5 M HCl without and with different concentrations of GDE at 25°C

System /concentration	E_{corr} (mV/SCE)	I_{corr} $\mu A/cm^2$	$-b_c$ mV/dec	b_a mV/dec	$\eta_{pol}\%$
Blank	-401	487	143	105	-
0.10 g/L	-404	364	139	88	25
0.50 g/L	-402	150	160	81	69
1.00 g/L	-403	92	168	78	81
2.00 g/L	-399	29	134	68	94
4.00 g/L	-395	27	137	60	94

Chapter III: Measurements and Discussions

According to Figure III.3 and Table III.2, we observe that in the presence of the inhibitor:

➤ The cathodic Tafel lines (b_c) are parallel, indicating that the addition of RSM does not alter the reduction of solvated protons at the surface of API 5L X70 steel, which primarily occurs via a charge transfer mechanism [3]. Moreover, the approximately constant values of the anodic Tafel slopes (b_a) suggest that GDE does not change the steel dissolution mechanism [4].

➤ The values of both anodic and cathodic partial currents decrease with increasing GDE concentration, indicating a reduction in corrosion rate.

This shift of both anodic and cathodic branches toward lower values is a result of the inhibition of the anodic and cathodic reactions of API 5L X70 steel by *Ghars Date Extract*.

➤ The corrosion potential values are only slightly shifted. Generally, if the shift in (E_{corr}) exceeds 85 mV compared to the uninhibited solution, the inhibitor can be considered either anodic or cathodic in nature [5]. In our study, the maximum shift was 17 mV in HCl medium, indicating that GDE acts as a mixed-type inhibitor in HCl.

III.2.2 Impedance measurements

The EIS (Electrochemical Impedance Spectroscopy) diagrams obtained for API 5L X42 steel in 0.5 M HCl solution at 20°C, both in the absence and presence of different concentrations of GDE, are shown in Figure III.4.

The values of the electrochemical parameters for the various concentrations of the GDE inhibitor, obtained through EIS for the corrosion of API 5L X70 pipeline steel in 0.5 M HCl solution, are summarized in Table III.4.

Analysis of these results reveals that:

➤ The diameters of the capacitive semicircles increase with increasing GDE inhibitor concentration, indicating that the inhibition efficiency is enhanced with higher GDE concentrations in the 0.5 M HCl medium.

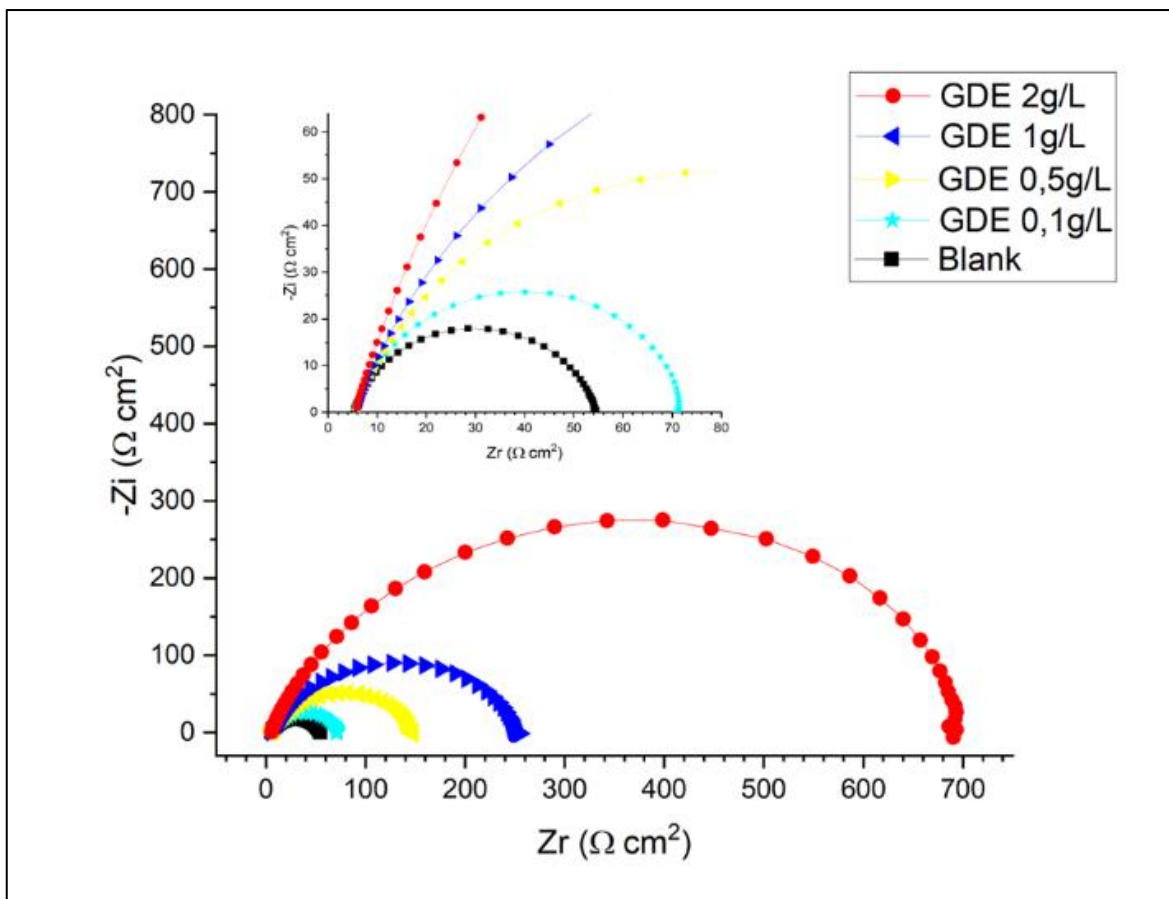


Figure III.4: EIS plots for API 5L X70 pipeline steel in 0.5 M HCl medium with and without different concentration of GDE at 20°C, Nyquist,

Chapter III: Measurements and Discussions

Table III.4: EIS plots for API 5L X70 pipeline steel 0.5 M HCl medium with and without different concentration of GDE at 20°C

System/concentration	R_s (Ωcm^2)	Y^0 ($\Omega\text{S}^n/\text{cm}^2$)	n	R_t (Ωcm^2)	C_{dl} ($\mu\text{F}/\text{cm}^2$)	$\eta_{\text{SIE}}\%$
Blank	5.1	350	0.8	49.46	134	-
0.10 g/L	5.4	209	0.83	66.83	103	26
0.50 g/L	5.5	163	0.79	142.20	75	65
1.00 g/L	5.5	131	0.82	248.00	70	80
2.00 g/L	5.5	80	0.82	685.00	50	93
4.00 g/L	5.6	75	0.82	690.00	45	93

➤ Increasing the inhibitor concentration also leads to an increase in charge transfer resistance (from 49 $\Omega\cdot\text{cm}^2$ to 685 $\Omega\cdot\text{cm}^2$) and a decrease in double-layer capacitance (from 134 $\mu\text{F}\cdot\text{cm}^{-2}$ to 50 $\mu\text{F}\cdot\text{cm}^{-2}$). This reduction is associated with the increased adsorption of RSM on the surface of API 5L X70 steel.

➤ The inhibition efficiency ($\eta_{\text{SIE}}\%$) increases with rising inhibitor concentration. It is worth noting that when the GDE concentration exceeds 1 g/L in 0.5 M HCl solution, the inhibition efficiency reaches a certain value (91%) and does not change significantly beyond that point.

➤ The inhibition efficiency increases with the inhibitor concentration, reaching 93% at 2g/L of GDE. The obtained values are consistent with those determined by electrochemical impedance spectroscopy (EIS)

Chapter III: Measurements and Discussions

➤ Figure (III.5) shows both the simulated and experimental impedance diagrams, along with the equivalent circuit, for API 5L X42 pipeline steel immersed in hydrochloric acid solution.

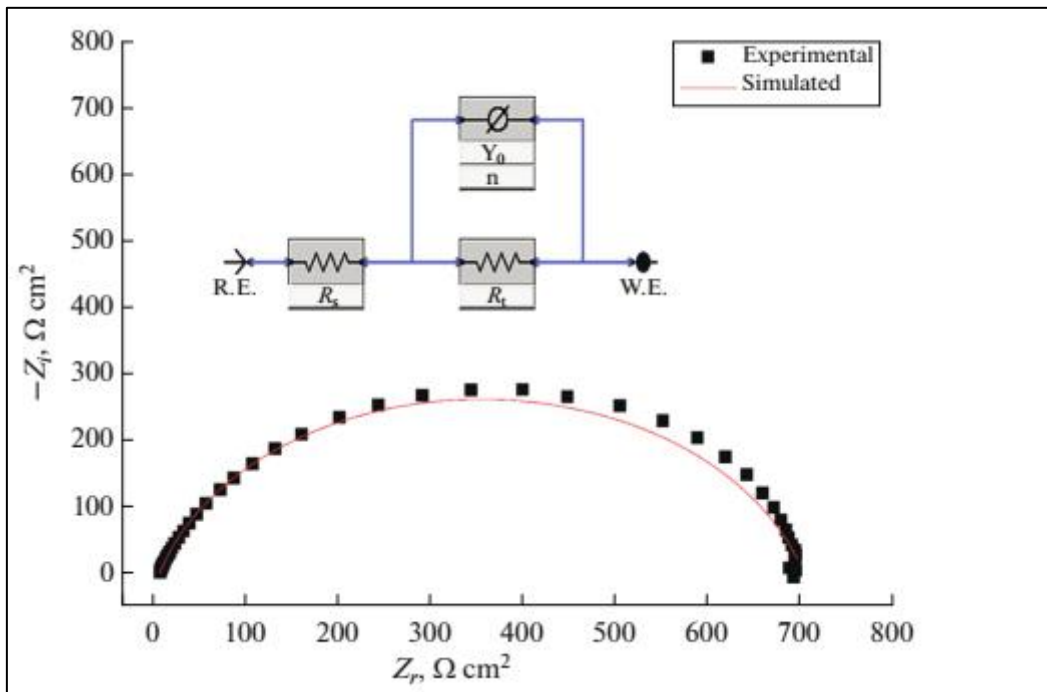


Figure (III.5): Simulated and experimental impedance diagrams of API5L X42 pipeline steel with equivalent circuit in hydrochloric acid medium

III.2.3 Adsorption Isotherm and Standard Free Energy of Adsorption of GDE on API 5L X70 Steel in HCl Medium

The surface coverage values (θ) for different concentrations of GDE inhibitor, obtained using the EIS method in 0.5 M HCl at 20°C, were used to test several adsorption isotherms—such as Langmuir, Frumkin, and Temkin—to determine which best describes the adsorption behavior of GDE. In this study, the Langmuir adsorption isotherm was found to best represent the adsorption process of GDE in 0.5 M HCl. The graphical representation of the Langmuir isotherm shows a linear relationship, with a regression coefficient very close to unity. This indicates that the adsorption of GDE on the steel surface at 20°C in 0.5 M HCl follows the Langmuir adsorption isotherm (Figure III.6).

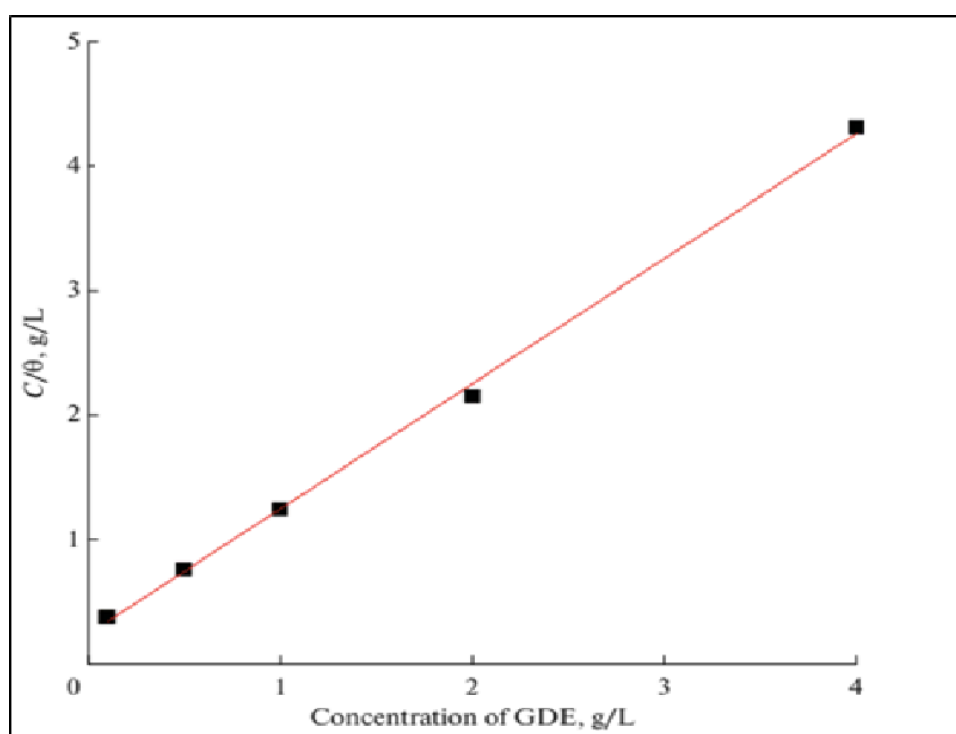


Figure (III.6): Langmuir adsorption isotherm of GDE on the surface of API 5L X70 steel in 0.5M HCl medium at 20 °C (obtained by the SIE method).

The current study evaluated various adsorption isotherms and found that the Langmuir adsorption isotherm most accurately described the adsorption behavior of the inhibitor under investigation (as shown in Figure III.6). This isotherm establishes a relationship between surface coverage ($\theta = \frac{\eta_{SIE}\%}{100}$) and inhibitor concentration (C) in the electrolyte [6], expressed by the following equation:

$$\frac{C}{\theta} = \frac{1}{K_{ads}} + C \quad (\text{Equ III.1})$$

The adsorption constant, K_{ads} , characterizes the adsorption process. A plot of C/θ versus C typically yields a straight line with a slope close to unity. From the value of K_{ads} , the standard free energy of adsorption (ΔG_{ads}^0) can be calculated using Equation (III.5) [6,7]:

$$\Delta G_{ads}^0 = -RT \ln(1 \times 10^6 K_{ads}) \quad (\text{Equ III.5})$$

Here, 1×10^6 represents the concentration of water in mg/L,

R is the universal gas constant,

T denotes the absolute temperature.

The corresponding values of ΔG_{ads}^0 and K_{ads} are presented in Table III.7. The magnitude of K_{ads} reflects the strength of interaction between the inhibitor molecules and the metal surface [8].

Typically, a ΔG_{ads}^0 value up to -20 kJ/mol indicates physical adsorption, which arises from electrostatic interactions between charged species. In contrast, values more negative than -40 kJ/mol suggest chemisorption, involving electron sharing or transfer to form coordinate bonds with the metal surface [9]. In this study, the calculated ΔG_{ads}^0 was -9.99 kJ/mol, indicating that the adsorption of GDE onto the API 5L X70 pipeline steel surface predominantly follows a physical adsorption mechanism. This finding aligns with observations reported by Ebenso et al[10].

Table III.5: Langmuir adsorption isotherm parameters for API 5L X70 pipeline steel in 0.5 M HCl solution containing GDE

Isotherm model	Linear correlation coefficient	Slope	K(L/g)	ΔG_{ads}^0 KJ/mol
Langmuir	0.99931	1.003	4.027	-9.99

III.2.4 Analysis of the surface of API 5L X70 steel by SEM in HCl medium without and with the GDE inhibitor

Figure III.11 presents microscope images and corresponding chemical analyses of polished metal samples, both with and without the GDE inhibitor, to illustrate the effectiveness of GDE as assessed through Electrochemical Impedance Spectroscopy (EIS) and polarization curve techniques. Upon immersion of API 5L X70 pipeline steel in hydrochloric acid, a corrosion product was observed forming on the metal surface (Fig. III.7.a), indicative of active corrosion.

Chapter III: Measurements and Discussions

In contrast, microscopy images of samples exposed to the inhibitor (Fig. III.7.b) show a clean surface with no visible corrosion products. Energy-dispersive X-ray spectroscopy (EDX) was used to analyze the surface composition of the API 5L X70 steel after 72 hours of exposure to 0.5 M hydrochloric acid (Table III.6). In the absence of GDE, the EDX spectra displayed prominent peaks for oxygen and chloride, confirming the presence of corrosion products. However, in the presence of 2 g/L GDE, the spectra revealed a marked reduction in oxygen and chloride content, suggesting that the inhibitor effectively adsorbed onto the steel surface and suppressed corrosion processes.

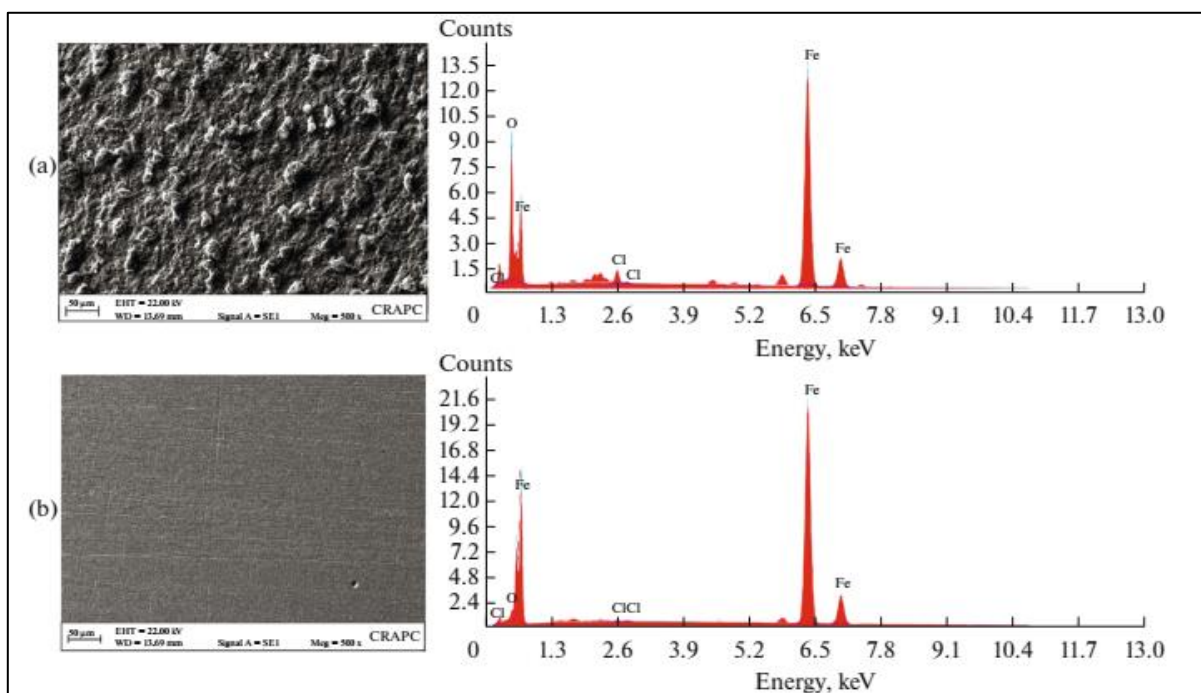


Figure III.7: SEM images of API 5L X70 pipeline steel in 0.5 M HCl at 20°C before and after 72 h immersion: (a) in 0.5 M HCl without inhibitor and (b) in 0.5 M HCl with 2 g/L GDE.

Table III.6 Content of elements obtained from EDX spectra for API 5L X70 pipeline steel

Element	at %	
	Steel + 0.5M HCl	Steel + 0.5M HCl + 2g/L GDE
Iron	60.37	95.54
Oxygen	37.62	04.06
Chlorine	02.00	00.40

The reduction in oxygen content and the increase in iron content indicate that in the presence of the GDE inhibitor, iron oxide (corrosion) does not form. These surface analysis results confirm the electrochemical findings

References

1. C.G. E. S. Ferreira, F. C. Giacomelli, A. Spinelli, Evaluation of the inhibitor effect of l-ascorbic acid on the corrosion of mild steel, *Materials Chemistry and Physics*, (2004) 129-134.
2. S.D. X. Li, H. Fu, Synergism between red tetrazolium and uracil on the corrosion of cold rolled steel in H₂SO₄ solution, *Corrosion Science*, (2009) 1344-1355.
3. I. Ahamad, R.P., and M. Quraishi, Thermodynamic, electrochemical and quantum chemical investigation of some Schiff bases as corrosion inhibitors for mild steel in hydrochloric acid solutions. *Corrosion Science*, 2010: p. 933-942.
4. M. Behpour, S.G., M. Khayatkashani, and N. Soltani, The effect of two oleo-gum resin exudate from *Ferula assa-foetida* and *Dorema ammoniacum* on mild steel corrosion in acidic media. *Corrosion Science*, 2011. **53**: p. 2489-2501.
5. X. Li, S.D., and H. Fu, Synergism between red tetrazolium and uracil on the corrosion
6. Sotelo-Mazon, O., et al., Corrosion protection of 1018 carbon steel using an avocado oil-based inhibitor. *Green Chemistry Letters and Reviews*, 2019. **12**: p. 255-270.
7. Solomon, M., S. Umoren, A. Israel, and I. Etim, Synergistic inhibition of aluminium corrosion in H₂SO₄ solution by polypropylene glycol in the presence of iodide ions. *Pigment and Resin Technology*, 2016. **45**.
8. Umoren, S.A., Polypropylene glycol: A novel corrosion inhibitor for ×60 pipeline steel in 15% HCl solution. *Journal of Molecular Liquids*, 2016. **219**: p. 946-958.
9. Bentrach, H., Y. Rahali, and A. Chala, Gum Arabic as an eco-friendly inhibitor for API 5L X42 pipeline steel in HCl medium. *Corrosion Science*, 2014. **82**: p. 426–431.
10. Ebenso, E., N. Eddy, and A. Odiongenyi, Corrosion inhibition and adsorption properties of methocarbamol on mild steel in acidic medium. *Portugaliae Electrochimica Acta*, 2009. **27**(1): p. 13-22.

General Conclusion

[General Conclusion]

The main objective of this thesis was to evaluate the inhibitory properties of a natural compound proposed for use as a corrosion inhibitor in the petroleum industry, with no harmful impact on the environment or human health. To this end, the corrosion inhibition efficiency of Ghars Date Extract was primarily assessed through electrochemical measurements. This product was chosen due to its non-toxicity, biodegradability, low cost, and easy availability from renewable sources.

The first aim of this work was to gain a better understanding of the corrosion behavior of API 5L X70 steel in hydrochloric acid, in order to then evaluate the inhibition properties of *Ghars Date Extract*

The main conclusions of this thesis can be summarized as follows:

1. The types of corrosion observed for API 5L X70 steel in 0.5 M HCl are uniform corrosion and pitting corrosion.
2. The optimal concentration of the GDE inhibitor was found to be 1 g/L, at which the corrosion rate decreased from 755 to 84 $\mu\text{A}/\text{cm}^2$.
3. The Tafel slope constants, ba and bc , remain unchanged in the presence of GDE.
4. Beyond the optimal concentration, the corrosion rate does not significantly change.
5. The adsorption of GDE on the API 5L X70 steel surface follows the Langmuir adsorption isotherm.
6. The standard free energy of adsorption indicates that the adsorption of GDE is physical in nature.
7. Potentiodynamic polarization results show that GDE acts as a mixed-type inhibitor.
8. The inhibition mechanism of GDE is likely based on geometric blocking.
9. The Nyquist diagram shows a single capacitive loop in the presence of GDE.

For future work, it would be advisable to study the influence of hydrodynamic conditions, under the same experimental parameters, on the effectiveness of GDE.

[General Conclusion]

It would also be beneficial for this study to incorporate advanced surface characterization techniques such as X-ray Photoelectron Spectroscopy (XPS) and Raman Spectroscopy. These methods would provide more precise insights into the formation of corrosion products and their interaction with GDE, ultimately enhancing its corrosion protection capabilities.

Résume :

Durant les dernières décennies, il a été largement utilisé des composés (toxiques, cancérigènes, à des prix exorbitants) comme des inhibiteurs de corrosion dans l'industrie pétrolière pour les tubes en acier au carbone. Toutefois, en raison de leurs effets dévastateurs, de nombreuses études ont été consacrées au développement des revêtements organiques acceptables pour la santé et l'environnement. Il est certain que les composés organiques naturels vont émerger comme des inhibiteurs efficaces de corrosion dans les années à venir grâce à leur bonne biodégradabilité, disponibilité facile et nature non toxique. Une lecture attentive de la littérature montre clairement que l'ère des inhibiteurs verts a déjà commencé. Ghars Date Extrait a été sélectionnée pour la présente étude.

Abstract :

In recent decades, many toxic, carcinogenic and expensive compounds were most commonly used as corrosion inhibitors in the petroleum industry for carbon steel tubes. However, due to their devastating effects, many studies have been devoted to developing acceptable organic coatings for health and the environment. It is certain that natural compounds emerge out as effective inhibitors of corrosion in the coming years due to their biodegradability, easy availability and non-toxic nature. Careful perusal of the literature clearly reveals that the era of green inhibitors has already begun. Ghars Date Extract was selected for the present study.

ملخص

في العقود الأخيرة، تم استخدام و بشكل واسع عناصر (سامة و مسرطنة و باهظة الثمن بالإضافة إلى عدم تحللها في الطبيعة بعد استخدامها) كمتبطات لتآكل الأنابيب (المصنوعة من الصلب الكربوني) المستخدمة في ميدان الصناعة البترولية. لكن، بسبب التأثير المدمر لهذه العناصر، توجهت الدراسات نحو البحث عن مركبات طبيعية مقبولة من الناحية الصحية و البيئية و الاقتصادية. من الأكد أن المركبات العضوية الطبيعية سوف تظهر كمتبطات فعالة للتآكل في السنوات القادمة بسبب تحللها البيولوجي الممتاز و توفرها في كل مكان و بتميزها بعدم السمية. الدراسة المتنتية للأبحاث المنشورة حول استخدام المركبات الطبيعية كمتبطات للتآكل تثبت بشكل واضح أن عصر ما يسمى بالمتبطات الخضراء قد بدأ فعلا. في هذه الدراسة تم اختيار مستخلص عسل التمر.